Published in final edited form as:
Toxicology. 2017 March 01; 378: 25–36. doi:10.1016/j.tox.2017.01.001.

Comparison of fluorescence-based methods to determine nanoparticle uptake by phagocytes and non-phagocytic cells in vitro

Meindl Claudia[a], **Öhlinger Kristin**[a], **Ober Jennifer**[a], **Roblegg Eva**[b], and **Fröhlich Eleonore**[a,*]

[a]Center for Medical Research, Medical University of Graz, Stiftingtalstr. 24, 8010 Graz, Austria

[b]Institute of Pharmaceutical Sciences, Department of Pharmaceutical Technology, Karl-Franzens-University of Graz, Humboldtstr, 46, 8010 Graz, Austria

Abstract

At many portals of entry the relative uptake by phagocytes and non-phagocytic cells has a prominent effect on availability and biological action of nanoparticles (NPs). Cellular uptake can be determined for fluorescence-labeled NPs. The present study compares three methods (plate reader, flow cytometry and image analysis) in order to investigate the influence of particle size and functionalization and medium content on cellular uptake of fluorescence–labeled polystyrene particles and to study the respective method's suitability for uptake studies. For comparison between the techniques, ratios of macrophage to alveolar epithelial cell uptakes were used. Presence of serum protein in the exposure solution decreased uptake of carboxyl-functionalized and non-functionalized particles; there was no clear effect for the amine-functionalized particles. The 200 nm non- or carboxyl-functionalized NPs were taken up preferentially by phagocytes while for amine-functionalized particles preference was lowest. The presence of the serum slightly increased the preference for these particles.

In conclusion, due to the possibility of calibration, plate reader measurements might present a better option than the other techniques to (semi)quantify differences between phagocytes and non-phagocytic cells for particles with different fluorescence. In order to obtain unbiased data the fluorescent labeling has to fulfill certain requirements.

Keywords

Phagocytes; Nanoparticles; Cellular uptake; Exposure conditions; Inhalation exposure

*Corresponding author at: Center for Medical Research, Medical University of Graz, Stiftingtalstr. 24, A-8010, Graz, Austria. eleonore.froehlich@medunigraz.at.

Competing interests
The authors declare that they have no competing interests.

Europe PMC Funders Author Manuscripts

1 Introduction

In human tissues, phagocytes and non-professional phagocytes are located in close vicinity. Phagocytes are part of the mononuclear phagocyte system (MPS), also called reticuloendothelial system. These cells play an important role in the uptake of foreign materials, pathogens and damaged cells. The extent of their phagocytic activity can influence concentrations of particles, including nanoparticles (NPs), at epithelial barriers and in tissues. Cellular uptake is linked to biological effects as well as to cytotoxicity (Sabella et al., 2014) and influenced by several parameters. Binding of macromolecules to the particle surface (‘protein corona’) has been identified as main determinant of biological effects (Rahman et al., 2013) and many studies were dedicated to the characterization of medium-specific composition, time dependence, and dynamic structure of the protein corona. These studies, however, were not able to predict qualitative and quantitative differences in the cellular uptake, making uptake measurements in the given exposure condition necessary.

Size, shape and surface properties are the most decisive particle-related parameters for cellular uptake and might influence the relation of phagocyte to non-phagocte uptake (Li, 2014). Cellular uptake in vitro is influenced by medium composition, particularly by the protein content, and by exposure conditions, e.g. particle concentrations, height of the medium on top of the cell layer, and perfusion with medium. Biological parameters that influence particle uptake include cell size, proliferation rate, growth pattern and expression of uptake routes (Fröhlich et al., 2012; Rees 2013).

An important area for both therapeutic interventions and environmental exposure is the alveolar region of the lung where alveolar epithelial cells and macrophages are localized. Particle uptake by alveolar macrophages together with removal by mucus through mucociliary clearance represents the main clearance mechanism in the deep lung (Tomashefski and Farver, 2008). Phagocytes, such as alveolar or peritoneal macrophages, and non-phagocytic cells, such as epithelial cells, differ in their ability to ingest particles. Alveolar macrophages preferentially phagocytize particles of 3–6 μm size (Hirota et al., 2007) but may also ingest NPs to higher rate than non-phagocytes. The pinocytosis rate of murine fibroblasts is 18.7 μm^3/h/cell compared to 46.5 μm^3/h/cell in murine peritoneal macrophages (Edelson et al., 1975; Steinman et al., 1974). NPs of various materials have been localized inside cells (polystyrene: (Kuhn et al., 2014; Schimpel et al., 2015); silica: (Kasper et al., 2013); quantum dots: (Chakraborty and Jana, 2015)) but quantitative data as well as systematic comparisons of particle uptake between different cell types are scarce. This is mainly due to lack of appropriate quantification methods or problems in the differentiation between intact particles and dissolved particles in the case of several metal and metal oxide NPs. Furthermore, the differentiation between plasma membrane-bound and ingested particles poses problems. The contribution of extracellular fluorescence to the signal obtained by flow cytometry was estimated as 30% in one study (Vranic et al., 2013). As for many other biological readout parameters of NP action there are no standardized protocols for the measurement of uptake. Therefore, the researchers are using different methods and it is not clear if the different techniques provide the same information. The establishment of Standard Operation Procedures (SOPs) for NP testing is the aim of several European projects, for instance of NanoDiaR (Roubert et al., 2016). In order to evaluate

existing protocols for their suitability as SOP several parameters, such as requirements from the particle side, influencing factors, and obligatory controls have to be known.

With the overall aim to suggest one strategy for the quantification of cellular uptake of fluorescence-labeled particles, this study investigated the influence of particle parameters (size, surface functionalization) and exposure conditions (medium, culture) on particle uptake by phagocytes and epithelial cells by different methods. Pulmonary exposure was mimicked and fluorescence-labeled 20 nm and 200 nm non-functionalized plain (PPS20 and PPS200), carboxyl-functionalized (CPS20 and CPS200) and amine-functionalized (AMI20 and AMI200) polystyrene particles were used as models. Exposure conditions were kept constant for all evaluation methods. Alveolar lining fluid and plasma contain serum albumin and immunoglobulin as major components (Kim and Malik, 2003). Fetal bovine serum (FBS) content of the exposure solution was chosen based on protein content between 1.3 mg/ml and 5.3–9 mg/ml in the alveolar lining fluid (Fick et al., 1984; Olsson et al., 2011) and 32–70 mg/ml protein in FBS preparations (Lindl, 2002). Human A549 alveolar epithelial cells were chosen as representatives for epithelial cells and DMBM-2 murine macrophages for phagocytes. A549 cells are frequently used in studies on pulmonary toxicity, while they are less suitable for studies on the alveolar barrier function (see for instance (Akhtar et al., 2012; Fröhlich et al., 2013; Lankoff et al., 2012; Stoehr et al., 2011)). Murine macrophages phagocytize particles similarly to human macrophages but behave more homogenous in culture (Gantt et al., 2001). In addition to monocultures also co-cultures of both cell types were studied. Co-culture of human and murine cells are used in several fields of research, particularly in the study of stem cell differentiation. The murine cells induce similar physiological reactions in human cells but are less efficient than the human counterparts (Matsuzaki et al., 1999; Reichert et al., 2015; Stecklum et al., 2015).

2 Methods

2.1 Particles

Red carboxyl-functionalized particles 20 nm and 200 nm (FluoSpheres® carboxylate-modified microspheres, Invitrogen), 20 nm amine-functionalized particles (green dyed Estapor F2-XC, Merck Millipore), 200 nm red amine-functionalized particles (FluoSpheres® amine-modified microspheres, Invitrogen) and non-functionalized 20 nm and 200 nm red dyed polystyrene particles (Fluoro-Max R25 and R200, ThermoScientific) were used.

2.2 Particle characterization

Hydrodynamic size and zeta potential were determined in particle suspensions with a concentration of less than 1 mg/ml. The particles were suspended in DMEM with 0% FBS, 2% FBS or 10% FBS and put into an Elmasonic S40 water bath (ultrasonic frequency: 37 kHz, Elma) for 10 min. Particles were measured via photon correlation spectroscopy (PCS, Malvern Zetasizer, Malvern Instruments) equipped with a 532 nm laser. The zeta potential was measured by Laser Doppler Velocimetry (scattering angle of 17°) coupled with Photon Correlation Spectroscopy (Zetasizer Nano ZS, Malvern Instruments, Malvern, UK) and calculated out of the electrophoretic mobility by applying the Henry equation. It has been reported that agglomerates of amine-functionalized in contrast to other polystyrene particles

after 24 h at 37 °C differed from the initial size (Paget et al., 2015). Therefore, particle sizes were determined at the start of the incubation and after 24 h at 37 ° C in the different exposure media.

To identify the presence of free dye in the solution, fluorescence of freshly prepared suspensions were measured. Particle suspensions (20 μg/ml) in medium + 0% FBS were used and fluorescence of serial dilutions of the suspensions measured (FLUOstar Optima, BMG Labortechnik) with the Ex/Em wavelengths (584/612 nm, CSP20, CPS200, AMI200; 544/612 nm, PPS20, PPS200; 485/520 nm, AMI20). After centrifugation at 220,000*g* in an OPTIMA L-90k ultracentrifuge (Beckman Coulter) for 60 min fluorescence of the supernatants were determined. Alternatively, particle suspensions were filtered through a 0.1 μm syringe filter (Minisart® 0.1 μm, Sartorius) and fluorescence in the filtrate compared to that of the non filtrated suspension.

2.3 Cell culture

DMBM-2 mouse macrophages and A549 cells (derived from a human lung adenocarcinoma) were obtained from Deutsche Sammlung für Mikroorganismen und Zellkulturen GmbH. DMBM-2 cells were cultured in Dulbecco's Modified Eagle's Medium (DMEM) supplemented with 20% horse serum, 2 mM L-glutamine and 1% penicillin/streptomycin. A549 cells were cultured in DMEM, 10% fetal bovine serum (FBS), 2 mM L-glutamine and 1% penicillin/streptomycin. Cells were sub-cultured at regular intervals.

Cells in monocultures ($2*10^5$ DMBM-2 and $1*10^5$ A549 per well) were seeded 24 h before treatment in 12-well plates in their cell-specific medium for plate reader and flow cytometry. Different cell densities had to be used to generate the sub-confluent exposure condition needed because DMBM-2 cells are markedly smaller than A549 cells.

For image analysis cells were seeded in chamber slides. $8*10^4$ A549 cells were seeded per chamber (Nunc® Lab-Tek® Chamber Slide™ system) and cultured for 5 days prior to the addition of $4*10^4$ DMBM-2 macrophages. The co-culture was continued for 24 h and exposed to the particles. Macrophages were added in lower number of $4*10^4$ cells in order to obtain the physiological situation in the alveoli, where epithelial cells outnumber macrophages by a factor of 5 (Stone et al., 1992). In addition, cultures with $4*10^5$ cells/chamber were studied. At these densities DMBM-2 cells form confluent monolayers and the exposure is similar to the plate reader and flow cytometry experiments.

Particle suspensions were freshly prepared from stock solutions in DMEM with different contents (0% −2% −10%) of FBS and suspensions were put into an Elmasonic S40 water bath (ultrasonic frequency: 37 kHz, Elma) for 20 min prior to cell exposures. Cells were incubated with 2, 5 or 20 μg/ml of the fluorescence-labeled polystyrene particles prepared from the same stock solution used for the physicochemical characterization for 24 h at 37 °C. Medium was removed and cells were rinsed three times with medium. To exclude differences in diffusion and sedimentation between the different culture vessels due to different growth areas (12-well culture plate: growth area 3.6 cm^2, 6-well transwell: growth area 4.6 cm^2, chamber of 4-chamber slide: growth area 1.7 cm^2) particles were added in an

amount of volume that provided the same height of working volume/growth area ratio. This was done in order to obtain similar diffusion distances.

2.4 Measurement in plate reader

To differentiate between active uptake and adhesion to the plasma membrane, cells were in parallel incubated with the particles in the presence of 50 mM sodium azide at 4 °C for 1 h. Longer incubation times were avoided because azide treatment interferes with mitochondrial respiration and causes cell alteration and cytotoxicity at higher doses and longer incubation times (Duewelhenke et al., 2007; Jones et al., 1980; Slamenova and Gabelova 1980). Kuhn et al. observed uptake of polystyrene particles already after 5–10 min of exposure and limited the exposure studies with inhibitors to 1 h (Kuhn et al., 2014).

Cells were removed from the wells by trypsin treatment and fluorescence was read at Ex/Em wavelength of 584/612 nm (CPS20, CPS200, AMI200), 544/612 nm (PPS20, PPS200) and 485/520 nm (AMI20), in a new plate using a fluorescence plate reader (FLUOstar Optima, BMG Labortechnik). Cell numbers and viability were determined with CASY TT Cell Counter and Analyzer System (Inovatis) to determine the amount of particles ingested per cell and to normalize uptake data in cells with and without uptake inhibition. Viability measurements served to identify potential effects of the different media. A standard curve was prepared using the solutions that had been added as stock solution and diluting them with cell suspensions to account for interference of the cells with the fluorescent signal. The stock solutions used for the standard curve were kept at 37 °C for the incubation time of 24 h.

2.5 Measurement by flow cytometry

After exposure to the particles in 12-well the cells were removed from the plastic support by trypsin treatment, rinsed in PBS and analyzed by flow cytometry performed on a FACS Aria flow cytometer using BD FACS Diva 8.0.1 software for data acquisition (BD Biosciences). The same gating was used for the particles in the two different media and ten thousand cells of each sample were analyzed.

2.6 Measurement by image analysis

All cultures (mono- and co-cultures) were exposed to particles for 24 h. Medium was removed, cells rinsed in medium and fixed for 15 min in 4% paraformaldehyde. Immunoreactivity against F4/80 antigen was performed to unequivocally identify DMBM-2 cells in co-culture with A549 cells. For detection the fixative was removed by three rinses with PBS and slides incubated with Alexa Fluor® 647 anti-mouse F4/80 (rat IgG2a, kappa, 1:500, Biozym) antibody for 30 min at RT, followed by three rinses in PBS and counterstain of nuclei with 1 μg/ml Hoechst 33342. Slides were viewed in a confocal Laser Scan microscope (LSM510 Meta, Zeiss) and images were taken at two different planes of the co-cultures; the plane of the DMBM-2 and the one of the A549 cells. Images were analyzed according to brightness in the different channels using ImageJ (1.49 v, National Institutes of Health) software. For comparison with low density of macrophages individual cells and cell groups were analyzed (50 cells/exposure). For the experiments where A549 and DMBM-2 cells were seeded at high confluency, areas of the slide were evaluated. The same particle-

specific microscope setting was used for the medium-dependent comparisons of the uptake. For each particle 202.500 μm^2 were evaluated this way.

Intercellular uptake of particles was differentiated from adhesion to the plasma membrane by staining of the actin cytoskeleton with fluorescence-labeled phalloidin. After particle incubation and washing of the cells with prewarmed PBS, cells were fixed for 10 min at RT with 4% paraformaldehyde. Subsequently, cells were rinsed 3 times with PBS, permeabilized with acetone at −20 °C for 3 min, rinsed again in PBS, and 165 nM of fluorescence-labeled phalloidin was added for 20 min at RT. Alexa Fluor® 488-phalloidin was used in combination with red particles and Alexa Fluor® 633 phalloidin (Invitrogen) in combination with green particles. After 3 final rinses in PBS cells were viewed in an A1R Laser Scan microscope (Nikon) at ex/em of 488 nm and 518 nm. For each condition microscope setting for optimal detection were used.

2.7 Cytotoxicity testing

Viability was assessed as formazan bioreduction by cellular dehydrogenases using a water-soluble tetrazolium salt (CellTiter 96® Aqueous Non-Radioactive Cell Proliferation Assay, Promega). After incubation to the particles, medium was removed and the combined MTS/PMS solution (200 µl + 1 ml medium) was added to all wells. Plates were incubated for 2 h at 37 °C in the cell incubator. Absorbance was read at 490 nm on a plate reader (Spectrostar Omega, BMG Labtech). To correct for absorbance by the polystyrene particles alone, the signal of MTS/PMS + particles (in the absence of cells) was subtracted. All values are referred to medium-exposed cells as 100%.

2.8 Statistics

Data were subjected to statistical analysis and are represented as means ± S.D. Data were analyzed with one-way analysis of variance (ANOVA) followed by Tukey-HSD post hoc test for multiple comparisons (SPSS 19 software). Nonparametric data were analyzed with ANOVA on Ranks followed by Dunn’s post hoc test. Results with p-values of less than 0.05 were considered to be statistically significant.

3 Results

3.1 Characterization of the particles

In order to compare particle uptake by different fluorescent techniques several parameters have to be determined: size and surface charge of the particles and intensity and stability of the included dye. Concentration-dependency of the uptake rate has to be determined since different methodologies might require exposure to different doses for optimal detection. Furthermore, size, agglomeration and surface charge of the particles have to be known for interpretation of the results.

Particles with nominal sizes of 20 nm and 200 nm had greater hydrodynamic size when suspended in cell culture medium (DMEM) with FBS than without FBS (Table 1). Multimodal distribution with 70% of the particles of small size and 30% forming agglomerates was seen for AMI20 in all culture media and for CPS200 particles in medium

+10% FBS. AMI200 particles were the only particles that formed larger agglomerates in all culture media. However, these agglomerates became smaller during the incubation at 37 °C (Table 1). Zeta potential values of CP200, PPS20, PPS200 and AMI200 particles were (–12) ± (–1) mV with no obvious trend regarding protein content. Only AMI20 particles (–24 mV) and CPS20 particles (–42 mV) showed negative values when suspended in DMEM +0%FBS (Fig. 1s, Supplementary material).

Fluorescence intensities of the particles were compared at the same gain setting in the plate reader. Compared to particles with the lowest fluorescence intensities (AMI20 and PPS20) suspensions of PPS200 particles showed 5.8–9.7 times, CPS200 particles 6.5–12.7 and AMI200 particles 12.0–13.1 times higher fluorescence (Fig. 1s, Supplementary material).

Unbound dye was detected by ultracentrifugation and filtration to identify free dye in the particle solution that might limit interpretation of the measurements. The procedure could be used for the 200 nm particles and 2.7 ± 0.9% (CPS200), 4.9 ± 1.1% (PPS200) and 4.9 ± 0.7% (AMI200) of the signal remained in the supernatant. When filtration with 0.1 μm pore size was used between 0.05 ± 0.001% (CPS200), 0.03 ± 0.001% (PPS200) and 0.07 ± 0.002% (AMI200) of the original fluorescence was measured in the filtrate.

As slightly different particle concentrations were used to allow optimal detection by the respective techniques, concentration dependence between 2 μg/ml and 20 μg/ml was evaluated. There was no significant trend for higher%uptake upon incubation with higher particle concentrations. 10^5 A549 cells in the culture for instance ingested between 1.9–4.8% (CPS20), 3.5–6.7% (CPS200), 1.4–4.0% (PPS20), 3.7–5.5% (PPS200), and 4.6–8.3% (AMI200) of the added particles independent of the particle concentration when applied in DMEM + 0% FBS (data not shown).

To find out whether murine macrophages were activated in the co-cultures, immunoreactivity for the F/80 antigen was compared in mono- and co-culture using flow cytometry. Phagocytosis by macrophages is induced by opsonization with autologous serum compounds, immunoglobulins and complement factors, but can also occur in the absence of opsonization. The F4/80 antigen is expressed on murine macrophages and a marker for red pulp splenocytes that eliminate red blood cells from the circulation (Mosser and Zhang 2011; Sano et al., 1980; Sugimoto et al., 1980; Wang et al., 2013). The median did not differ between monocultures of DMBM-2 cells and co-culture with A549 cells and was 6515 ± 199 artificial fluorescence units (AFU) in the monocultures and 6536 ± 378 AFU in co-cultures with A549 cells.

3.2 Cytotoxicity

Prior to the uptake experiments cell viability and cell number were determined to identify potential influence of the serum and of the tested NPs. Absence of FBS for 24 h did not significantly decrease viability. Absorbance values were 2.39 ± 0.25 in DMEM + 0% FBS vs. 2.79 ± 0.38 in DMEM + 10% FBS for A549 cells and 1.03 ± 0.07 in DMEM + 0% FBS vs. 1.23 ± 0.16 in DMEM + 10% FBS for DMBM-2 macrophages. The respective cell numbers were 3.66 ± 0.4 vs. 4.26 ± 0.4 for A549 cells and 5.77 ± 1.3 vs. 5.9 ± 1.6 for DMBM-2 macrophages. Viability determined with electro-chemical sensing was 94.5

± 0.7% in DMEM + 0% FBS and 95.8 ± 0.8% in DMEM + 10% FBS for A549 cells and 90.8 ± 2.0% in DMEM + 0% FBS and 89.1 ±1.2% in DMEM + 10% FBS for DMBM-2 macrophages. None of the particles did decrease cell viability in concentrations <50 μg/ml (data not shown).

3.3 Considerations for the determinations by plate reader, flow cytometry, and image analysis

To compare particle uptake between different cell types and media composition plate reading was used and uptake indicated as pg/cell. The indication in weight/cell was preferred to particle number/cell because particle number was only given for the original solutions in water. Medium + FBS caused increases in particle size and agglomeration (Table 1) and consequently changed the number of single particles.

Due to low fluorescence the uptake of AMI20 particles could not be determined reliably with plate reader measurements. Uptake of PPS20 particles, which also possessed only a low fluorescence signal in the plate reader, could be determined although standard deviations in general were higher than for the other particles. Fluorescence was stable over the incubation time only for CPS20, CPS200, and PPS200 particles and, therefore, stock solutions kept at 37 °C for 24 h were used to calculate uptake data. For the comparison between all techniques particle uptake was determined in medium with 0% FBS and 10% FBS.

3.4 Particle uptake

3.4.1 Determination by plate reader—Cellular uptake was compared between the media and between the particles in a given medium. Data from AMI20 particles are not shown because the fluorescent signal was too low to enable reliable measurements with plate reader (Fig. 1s, Supplementary material). A549 cells showed marked differences in the uptake when particles were suspended in DMEM + 0% FBS compared to DMEM + 2% FPS (Fig. 1a), while differences between particle uptake in DMEM + 2% FBS and DMEM + 10% FBS were small. Uptake was significantly lower in FBS-containing media compared to DMEM + 0% FBS for all particles, except PPS20, where standard deviations were very high. Uptake of AMI200 particles was higher than uptake of the other particles, when suspended DMEM + 0% FBS, DMEM + 2% FBS, and DMEM + 10% FBS.

DMBM-2 macrophages were less affected by the FBS content of the medium. Only the uptake of PPS200 particles was significantly lower in DMEM + 10% FBS than in DMEM + 0% and DMEM + 2% FBS (Fig. 1b). When suspended in DMEM + 10% FBS differences in particle uptake was only significant between PPS200 and AMI200 particles.

Upon inhibition of active uptake by sodium azide, particle uptake rates in both cell lines and in both medium conditions were markedly decreased (Fig. 2). The remaining signal showed particle-specific differences. These uptake rates were higher in the exposure in DMEM + 0% FBS than in DMEM + 10% FBS and higher for non-functionalized (PPS20 and PPS200) particles than for functionalized particles (Fig. 2). The rates between the cell types were only significantly different for the non-functionalized PPS20 and PPS200 particles.

3.4.2 Determination by flow cytometry—The methodology enables the indication of the fraction of the cells that contained particles and the intensity of the fluorescence in these cells. Due to the different intensities in the fluorescence of the particles, comparisons of uptake between different particles are not possible. Only monocultures were assessed because the macrophage marker F4/80 interfered with signal of the particles. Using the same gating, uptake in different media was compared.

The percentage of A549 cells that ingested particles was >50% for CPS20, PPS200, AMI20 and AMI200 particles when applied in both media (a, Fig. 2s, Supplementary material). CPS200 and PPS20 particles, however, were ingested by a significantly lower fraction of cells in both media. Uptake of all particles, except PPS20 particles in DMEM + 10% FBS, was >50% by DMBM-2 cells (b, Fig. 2s, Supplementary material).

To reveal differences in particle uptake between media, median values were used, which showed that A549 cells ingested significantly more PPS200 particles and less AMI20 particles in DMEM + 0% FBS than in DMEM + 10% FBS (Fig. 3a).

Uptake of AMI20 particles in DMEM + 10% FBS was decreased in DMBM-2 macrophages compared to DMEM + 0% FBS (Fig. 3b).

3.4.3 Determination by analysis of microscopical images—This technique does not allow the comparison between different particles due to the differences in fluorescence but, when the same settings for image acquisition are used, uptake in different media can be compared. F4/80 labeling served to identify DMBM-2 macrophages in the co-cultures (Fig. 3s, Supplementary material). In one setting cells were seeded at densities resembling the situation in vivo with confluent epithelial cells and rare macrophages. Uptake in both cell types was also analyzed at high macrophage densities.

Particle uptake by A549 cells showed no significant differences between DMEM + 0% FBS and +10% FBS, except for amine-functionalized particles (Fig. 4a), which were ingested to higher extent in DMEM + 10% FBS medium. When DMBM-2 macrophages were seeded at low density (4×10^4 cells/chamber, Fig. 4b), CPS20 and PPS20 particles were taken up to a lower extent in DMEM + 10% FBS. Uptake data in co-cultures were similar to data generated in monocultures (data not shown). When uptake was analyzed at high density (4×10^5 cells/chamber, Fig. 4s, Supplementary material), DMBM-2 macrophages ingested particles with roughly the same preference as at low density, but significance levels were slightly different. At the high density seeding significantly less PPS200 particles and more AMI200 particles were ingested in DMEM + 10% FBS compared to DMEM + 0% FBS (Fig. 4s, Supplementary material, b). A549 cells ingested more AMI20 as in the evaluation at low macrophage seeding. The decreased uptake of PPS200 particles also observed in the low macrophage seeding condition was significant in these exposures (Fig. 4s, Supplementary material, a vs. Fig. 4a).

In order to find out whether the fluorescence signal in the plate reader experiments upon inhibition of active uptake was caused by particle adherence to the plasma membrane or by passive uptake of the particles, the cytoskeleton was stained with fluorescence-labeled

phalloidin. The images show mainly intracellular localization of all particles in both cell types. A549 cells were easier to analyze because of larger cell size and more distinct labeling of the cytoskeleton with phalloidin. Fig. 5 shows the comparison of the non-functionalized (PPS20 and PPS200) particles, which displayed a high signal after incubation with inhibitor (Fig. 2), to the carboxyl-functionalized particles with a low signal in the inhibitor experiments in both cell types. Data obtained in DMEM + 10%FBS are shown in Fig. 5s (Supplementary material).

3.5 Preferential uptake by macrophages according to the different detection methods

In order to find out if all techniques would identify the same particles as preferentially ingested by macrophages, the DMBM-2/A549 uptake ratios were calculated (Fig. 6). The range of the uptake ratio was much smaller for the plate reader than for flow cytometry and Image analysis. Therefore, a threshold of >1 for preferential uptake by macrophages was chosen for reader and a ratio >2 for the two other techniques. Highest preference for macrophage uptake in DMEM + 0% FBS was recorded for PPS20 particles by all techniques in addition to CPS20 particles according to reader and CPS200 particles by image analysis. In the exposures in DMEM + 10% FBSall techniques identified preferential uptake of CPS200 particles by the phagocytes. PPS20 and PPS200 particles also showed high uptake ratios, while the amine-functionalized particles AMI20 and AMI200 had the lowest preference for macrophage uptake. There were fewer matches in the identification of preferential uptake in DMEM + 0% FBS. One potential reason for different results could be the use of different particle concentrations. Therefore, the DMBM-2/A549 ratio determined at 20 μg/ml was compared to the ratio at 2 μg/ml and 5 μg/ml. No markedly different ratios were determined in this concentration range (Fig. 6s, Supplementary material, a). When a similar comparison was made for concentrations of 2 μg/ml and 5 μg/ml by flow cytometry generally slightly higher DMBM/A549 ratios were obtained for the higher concentration (Fig. 6s, Supplementary material, b). Nevertheless, these differences were not significant.

Preference for phagocyte uptake was significantly influenced by the medium composition for CPS200 and AMI20 particles. Uptake ratios in DMEM + 10% FBS were higher for CPS200 (plate reader and flow cytometry) and PPS200 particles (flow cytometry and image analysis) and lower for AMI20 particles (flow cytometry and image analysis).

4 Discussion

This study systematically investigated the influence of particle size and surface charge in different exposure media on cellular uptake. Different detection methods were compared with the aim to identify a standardized technique for the quantification of fluorescence-labeled particles. In order to apply particles in a realistic concentration range mass doses of 0.55–5.5 μg/ml were chosen. These doses are similar to exposures at the workplace, where concentrations of 0.14–1.57 μg/cm^2 were indicated for cellulose nanocrystals (Endes et al., 2014). Occupational exposure to carbon nanotubes and nanofibers reaches 0.24–2.4 μg/cm^2 (Chortarea et al., 2015). Interestingly, concentrations for inhalation treatment of pulmonary cancer are indicated in a similar range (0.5–0.86 μg/cm^2, (Kuzmov and Minko, 2015)).

Instability of the particle suspensions can influence particle uptake and was more pronounced for amine-functionalized particles than for carboxyl-functionalized and non-functionalized particles. Distribution of AMI20 particles was multimodal, while AMI200 particles formed one peak of agglomerates, which dissociated into smaller agglomerates after 24 h incubation in cell culture medium (Table 1). The lower stability of amine-functionalized polystyrene particles in protein containing medium has been reported by other groups and may be due not only to higher protein binding but also to the linking by counter ions, for instance phosphates, present in the cell culture medium (Kendall et al., 2015; Nasser and Lynch 2016; Xia et al., 2006). For cellular exposures it is important to note that the agglomerates break down during the incubation at 37 ° C.

The evaluation of the different detection techniques identified plate reader analysis as a promising candidate for standardized uptake studies because the signal of the uptake could be related to total fluorescence and particles with different fluorescence intensities could be compared. Compared to image analysis, plate reader and flow cytometry may provide a better analysis because a higher number of cells are studied. In order to obtain unbiased data the intensity of the labeling has to be high, the labeling has to be stable at 37 °C for 24 h, and there should be no free dye in the solution. The normalization to cell number is very important because cells have different sizes and uptake should be measured in confluent cultures because the cell cycle influences the uptake rate (Treuel et al., 2013). A shortcoming of plate reader measurements is the inability to evaluate co-cultures, which is generally possible in the other techniques. Another inherent problem is the restriction to fluorescent particles for imaging and plate reader analysis because the detection of colored particles is accompanied by a prominent loss in sensitivity. Limitation to the study of fluorescent particles is lowest in flow cytometry, where changes in side scatter of exposed and not exposed cells can be used to assess uptake of non-fluorescent particles, although also linked to a loss in sensitivity. All techniques share the limitation that no distinction is possible between ingested and plasma membrane bound particles. The combination of microscopy and flow cytometry, termed flow imaging, is an option to exclude plasma membrane-bound particles from the analysis. Vranic et al. studied cellular uptake of fluorescence-labeled silica NPs by bronchial epithelial cells using flow cytometry and flow imaging (Vranic et al., 2013). Although a direct comparison of the uptake rates by the different techniques is missing, the authors detected no plasma membrane-attached particles after incubation for 24 h at 37 ° C. This suggests that under the conditions chosen in our study the contribution of plasma membrane-bound particles is low, which corresponds to our microscopical analysis. We used the combination of inhibitor studies with plate reader and microscopy to quantify the contribution of plasma membrane bound particles and recorded a higher signal in the presence of inhibitors for non-functionalized compared to functionalized particles. Unchanged uptake of non-functionalized polystyrene particles in the presence of inhibitors has also been reported by Treuel et al. and the authors suggested a preference of the non-functionalized polystyrene particles for dynamin- and clathrin-independent mechanisms (Treuel et al., 2013). Based on our study non-functionalized polystyrene particles enter cells to a higher extent by passive uptake than the amine and carboxyl-functionalized particles. The interpretation of the experiments with PPS20 particles have to

be interpreted with caution since signals showed a high variation in the plate reader due to low fluorescence intensity.

Determination of the ratio between phagocytes and non-phagocytic cells is a good way to reduce method-inherent errors. The ratio between cells is also the information that is needed for toxicological interpretation to find out to which extent macrophages are damaged more than epithelial cells. This information is further important for the delivery of pharmaceutical compounds. Many compounds destined to be delivered to epithelial cells can be removed by phagocytes.

The inter-particle comparison showed that amine-functionalized particles were ingested to a greater extent by A549 cells than the other particles. The preferential uptake of charged NPs compared to non-functionalized particles by non-phagocytic cells has also been reported for iron oxide and polystyrene particles and functionalization with cationic ligands is used to increase cellular uptake for transfection (Fröhlich, 2012). This preference was noticed in DMEM + 0% FBS and DMEM + 10% FBS.

Since the identification of the prominent role of macromolecule binding (protein corona) for the biological action of NPs, particles have been studied in a variety of exposure media (Monopoli et al., 2011). NPs suspended in protein-containing medium are generally ingested by non-phagocytic cells to a lower extent and cause less cell damage (Fröhlich, 2012). Consistent with this assumption, A549 cells in this study contained a lower amount of particles in DMEM with FBS than in DMEM + 0% FBS. These differences were already detected at low protein concentrations (DMEM + 0% FBS versus DMEM + 2% FBS), while the increase from 2% FBS to 10% FBS had only a small effect. According to Lee et al. the high particle surface energy of NPs results in unspecific interactions with the plasma membrane, and binding of macromolecules to the particle surface decreases this effect (Lee et al., 2015). The prominent effect of low FBS concentrations can be explained by the fact that a thin layer of proteins can decrease surface reactivity to a sufficiently great extent. Furthermore also a low protein concentration can result in a saturated adherence to the particle surface. The decrease of cellular uptake was most pronounced for PPS200 and carboxyl-functionalized particles, while amine-functionalized particles were not affected (Figs. 1 and 3). Rather than a higher binding of protein to carboxylated surfaces, Lee et al. proposed changes in conformation of the bound molecules at the particles surface as main reason for differences between positively and negatively charged NPs (Lee et al., 2015). The situation is different for phagocytes where binding of serum compounds results in higher uptake of 2–4.5 μm polystyrene particles (Champion et al., 2008). This was not the case in our study, where uptake of all particles by DMBM-2 macrophages was decreased in DMEM + 10% FBS (Figs. 1, 3, 5). Opsonization of particles is most effective for particles of 2–3 μm (Champion et al., 2008) and the NPs in this study were too small (<500 nm) to trigger phagocytosis. In addition to that, particle opsonization with bovine immunoglobulins and complement factors in FBS are expected to act less well than autologous (murine) serum. However, serum protein binding affected the DMBM-2/A549 uptake ratios. Although, in general, 10% FBS decreased particle uptake for both cell types, this effects was much smaller for DMBM-2 macrophages than for A549 cells. The trend for preferential uptake by macrophages was absent for 20 nm particles, which may correspond to the fact that they are

not targets for phagocytic uptake. Particles of 200 nm, by contrast, were better ingested by phagocytes compared to epithelial cells in the presence of a protein corona. This corresponds to the finding that 50–250 nm liposomes for targeting to epithelial cells have to be modified with poly(ethylene glycol) (PEG) to retard their uptake by phagocytes (Immordino et al., 2006).

5 Conclusion

Based on the comparisons between A549 and DMBM-2 macrophages, all measurement techniques (plate reader, flow cytometry and image analysis) identified preferential uptake of PPS200 and CPS200 particles in DMEM + 10% FBS by macrophages. The higher uptake of small amine-functionalized (AMI20) particles in DMEM + 10% FBS by A549 cells could also be identified by the different techniques. The analysis by plate reader was the most versatile tool because it allowed to semi-quantify uptake differences between the particles. The data showed that an unbiased assessment requires a careful characterization of the labeling and the normalization to cell number. Uptake measurements by flow cytometry and image analysis produced only relative values and need the comparison to a reference cell type. The coverage of particles with protein did not markedly influence the relative preference of particle uptake by cells (e.g. highest uptake of AMI200 particles by A549 cells) but increased the DMBM-2/A549 ratio for the 200 nm particles.

Appendix A. Supplementary data

Refer to Web version on PubMed Central for supplementary material.

Acknowledgements

This work was supported by the Austrian Science Fund grant P 22576-B18.

The support by Markus Absenger-Novak (image acquisition) and by Birgit Teubl (particle characterization) is gratefully acknowledged.

Abbreviations

A549	human lung adenocarcinoma epithelial cells
DMBM-2	murine macrophages
DMEM	Dulbecco minimal essential medium
FBS	fetal bovine serum
NPs	nanoparticles
CPS20 and CPS200	carboxyl-functionalized polystyrene, sizes 20 nm and 200 nm
AMI20 and AMI200	amine-functionalized polystyrene, sizes 20 nm and 200 nm
PPS20 and PPS200	plain polystyrene, sizes 20 nm and 200 nm

References

Akhtar MJ, Ahamed M, Khan MA, Alrokayan SA, Ahmad I, Kumar S. Cytotoxicity and apoptosis induction by nanoscale talc particles from two different geographical regions in human lung epithelial cells. Environ Toxicol. 2012; 29:394–406. [PubMed: 22331707]

Chakraborty A, Jana NR. Clathrin to lipid raft-endocytosis via controlled surface chemistry and efficient perinuclear targeting of nanoparticle. J Phys Chem Lett. 2015; 6:3688–3697. [PubMed: 26722743]

Champion JA, Walker A, Mitragotri S. Role of particle size in phagocytosis of polymeric microspheres. Pharm Res. 2008; 25:1815–1821. [PubMed: 18373181]

Chortarea S, Clift MJ, Vanhecke D, Endes C, Wick P, Petri-Fink A, Rothen-Rutishauser B. Repeated exposure to carbon nanotube-based aerosols does not affect the functional properties of a 3D human epithelial airway model. Nanotoxicology. 2015; 9:983–993. [PubMed: 25697181]

Duewelhenke N, Krut O, Eysel P. Influence on mitochondria and cytotoxicity of different antibiotics administered in high concentrations on primary human osteoblasts and cell lines. Antimicrob Agents Chemother. 2007; 51:54–63. [PubMed: 17088489]

Edelson PJ, Zwiebel R, Cohn ZA. The pinocytic rate of activated macrophages. J Exp Med. 1975; 142:1150–1164. [PubMed: 53258]

Endes C, Schmid O, Kinnear C, Mueller S, Camarero-Espinosa S, Vanhecke D, Foster EJ, Petri-Fink A, Rothen-Rutishauser B, Weder C, Clift MJ. An in vitro testing strategy towards mimicking the inhalation of high aspect ratio nanoparticles. Part Fibre Toxicol. 2014; 11:40. [PubMed: 25245637]

Fick RB Jr, Naegel GP, Squier SU, Wood RE, Gee JB, Reynolds HY. Proteins of the cystic fibrosis respiratory tract. Fragmented immunoglobulin G opsonic antibody causing defective opsonophagocytosis. J Clin Invest. 1984; 74:236–248. [PubMed: 6429195]

Fröhlich E, Meindl C, Roblegg E, Griesbacher A, Pieber TR. Cytotoxicity of nanoparticles is influenced by size, proliferation and embryonic origin of the cells used for testing. Nanotoxicology. 2012; 6:424–439. [PubMed: 21627401]

Fröhlich E, Bonstingl G, Hofler A, Meindl C, Leitinger G, Pieber TR, Roblegg E. Comparison of two in vitro systems to assess cellular effects of nanoparticles-containing aerosols. Toxicol In Vitro. 2013; 27:409–417. [PubMed: 22906573]

Fröhlich E. The role of surface charge in cellular uptake and cytotoxicity of medical nanoparticles. Int J Nanomed. 2012; 7:5577–5591.

Gantt KR, Goldman TL, McCormick ML, Miller MA, Jeronimo SM, Nascimento ET, Britigan BE, Wilson ME. Oxidative responses of human and murine macrophages during phagocytosis of Leishmania chagasi. J Immunol. 2001; 167:893–901. [PubMed: 11441096]

Hirota K, Hasegawa T, Hinata H, Ito F, Inagawa H, Kochi C, Soma G, Makino K, Terada H. Optimum conditions for efficient phagocytosis of rifampicin-loaded PLGA microspheres by alveolar macrophages. J Control Release. 2007; 119:69–76. [PubMed: 17335927]

Immordino ML, Dosio F, Cattel L. Stealth liposomes: review of the basic science, rationale, and clinical applications, existing and potential. Int J Nanomed. 2006; 1:297–315.

Jones JA, Starkey JR, Kleinhofs A. Toxicity and mutagenicity of sodium azide in mammalian cell cultures. Mutat Res. 1980; 77:293–299. [PubMed: 7383046]

Kasper J, Hermanns MI, Bantz C, Utech S, Koshkina O, Maskos M, Brochhausen C, Pohl C, Fuchs S, Unger RE, James Kirkpatrick C. Flotillin-involved uptake of silica nanoparticles and responses of an alveolar-capillary barrier in vitro. Eur J Pharm Biopharm. 2013; 84:275–287. [PubMed: 23183446]

Kendall M, Hodges NJ, Whitwell H, Tyrrell J, Cangul H. Nanoparticle growth and surface chemistry changes in cell-conditioned culture medium. Philos Trans R Soc Lond B Biol Sci. 2015; 370:20140100. [PubMed: 25533102]

Kim KJ, Malik AB. Protein transport across the lung epithelial barrier. Am J Physiol Lung Cell Mol Physiol. 2003; 284:L247–259. [PubMed: 12533309]

Kuhn DA, Vanhecke D, Michen B, Blank F, Gehr P, Petri-Fink A, Rothen-Rutishauser B. Different endocytotic uptake mechanisms for nanoparticles in epithelial cells and macrophages. Beilstein J Nanotechnol. 2014; 5:1625–1636. [PubMed: 25383275]

Kuzmov A, Minko T. Nanotechnology approaches for inhalation treatment of lung diseases. J Control Release. 2015; 219:500–518. [PubMed: 26297206]

Lankoff A, Sandberg WJ, Wegierek-Ciuk A, Lisowska H, Refsnes M, Sartowska B, Schwarze PE, Meczynska-Wielgosz S, Wojewodzka M, Kruszewski M. The effect of agglomeration state of silver and titanium dioxide nanoparticles on cellular response of HepG2, A549 and THP-1 cells. Toxicol Lett. 2012; 208:197–213. [PubMed: 22108609]

Lee YK, Choi EJ, Webster TJ, Kim SH, Khang D. Effect of the protein corona on nanoparticles for modulating cytotoxicity and immunotoxicity. Int J Nanomed. 2015; 10:97–113.

Li, M. Pharmacokinetics of polymeric nanoparticles at whole body, organ, cell, and molecule levels. Handbook of Research and Nanoscience, Nanotechnology, and Advanced Materials, Engineering Science Reference. Bououdina, M., Davim, J., editors. Hershey; 2014. p. 146-163.

Lindl, T. Zell- und Gewebekultur. Spektrum Akademischer Verlag; Heidelberg: 2002.

Matsuzaki K, Katayama K, Takahashi Y, Nakamura I, Udagawa N, Tsurukai T, Nishinakamura R, Toyama Y, Yabe Y, Hori M, Takahashi N, et al. Human osteoclast-like cells are formed from peripheral blood mononuclear cells in a coculture with SaOS-2 cells transfected with the parathyroid hormone (PTH)/PTH-related protein receptor gene. Endocrinology. 1999; 140:925–932. [PubMed: 9927325]

Monopoli MP, Walczyk D, Campbell A, Elia G, Lynch I, Bombelli FB, Dawson KA. Physical-chemical aspects of protein corona: relevance to in vitro and in vivo biological impacts of nanoparticles. J Am Chem Soc. 2011; 133:2525–2534. [PubMed: 21288025]

Mosser DM, Zhang X. Measuring opsonic phagocytosis via Fcgamma receptors and complement receptors on macrophages. Current Protocols in Immunology. 2011; Chapter 14:Unit 14.27.

Nasser F, Lynch I. Secreted protein eco-corona mediates uptake and impacts of polystyrene nanoparticles on Daphnia magna. J Proteomics. 2016; 137:45–51. [PubMed: 26376098]

Olsson, B., Bondesson, E., Borgström, L., Edsbäcker, S., Eirefelt, S., Ekelund, K., Gustavsson, L., Hegelund-Myrbäck, T. Pulmonary drug metabolism, clearence, and absorption. Controlled Pulmonary Drug Delivery. Smyth, H., Hickey, A., editors. Springer; New York: 2011. p. 21-50.

Paget V, Dekali S, Kortulewski T, Grall R, Gamez C, Blazy K, Aguerre-Chariol O, Chevillard S, Braun A, Rat P, Lacroix G. Specific uptake and genotoxicity induced by polystyrene nanobeads with distinct surface chemistry on human lung epithelial cells and macrophages. PLoS One. 2015; 10:e0123297. [PubMed: 25875304]

Rahman, M., Laurent, S., Tawil, N., Yahia, L., Mahmoudi, M. Nanoparticle and protein Corona. Protein-Nanoparticle Interactions The Bio-Nano Interface. Rahman, M.Laurent, S.Tawil, N.Yahia, L., Mahmoudi, M., editors. Springer; Heidelberg: 2013. p. 21-40.

Rees, P. Uptake and Toxicology of Nanoparticles. Nanomedicine. Summers, H., editor. Elsevier; Oxford: 2013.

Reichert D, Friedrichs J, Ritter S, Kaubler T, Werner C, Bornhauser M, Corbeil D. Phenotypic. morphological and adhesive differences of human hematopoietic progenitor cells cultured on murine versus human mesenchymal stromal cells. Sci Rep. 2015; 5:15680. [PubMed: 26498381]

Roubert F, Beuzelin-Ollivier M, Hofmann-Amtenbrink M, Hofmann H, Hool A. Nanostandardization in action: implementing standardization processes in a multidisciplinary nanoparticle-based research and development project. NanoEthics. 2016; 10:41–62.

Sabella S, Carney RP, Brunetti V, Malvindi MA, Al-Juffali N, Vecchio G, Janes SM, Bakr OM, Cingolani R, Stellacci F, Pompa PP. A general mechanism for intracellular toxicity of metal-containing nanoparticles. Nanoscale. 2014; 6:7052–7061. [PubMed: 24842463]

Sano K, Sugimoto M, Yasuda T, Egashira Y, Yamada M. Recognition of heterologous cells by macrophages. I. Species recognition by mouse and guinea pig macrophages in the phagocytosis of heterologous thymocytes. Microbiol Immunol. 1980; 24:957–967. [PubMed: 6970321]

Schimpel C, Rinner B, Absenger-Novak M, Meindl C, Fröhlich E, Falk A, Zimmer A, Roblegg E. A novel in vitro model for studying nanoparticle interactions with the small intestine. EURO-NanoTox Lett. 2015; 6:1–14.

Slamenova D, Gabelova A. The effects of sodium azide on mammalian cells cultivated in vitro. Mutat Res. 1980; 71:253–261. [PubMed: 7393241]

Stecklum M, Wulf-Goldenberg A, Purfurst B, Siegert A, Keil M, Eckert K, Fichtner I. Cell differentiation mediated by co-culture of human umbilical cord blood stem cells with murine hepatic cells. In Vitro Cell Dev Biol Anim. 2015; 51:183–191. [PubMed: 25270685]

Steinman RM, Silver JM, Cohn ZA. Pinocytosis in fibroblasts. Quantitative studies in vitro. J Cell Biol. 1974; 63:949–969. [PubMed: 4140194]

Stoehr LC, Gonzalez E, Stampfl A, Casals E, Duschl A, Puntes V, Oostingh GJ. Shape matters: effects of silver nanospheres and wires on human alveolar epithelial cells. Part Fibre Toxicol. 2011; 8:36. [PubMed: 22208550]

Stone KC, Mercer RR, Freeman BA, Chang LY, Crapo JD. Distribution of lung cell numbers and volumes between alveolar and nonalveolar tissue. Am Rev Respir Dis. 1992; 146:454–456. [PubMed: 1489139]

Sugimoto M, Sano K, Enomoto T, Yamada M, Egashira Y. Recognition of heterologous cells by macrophages. II. The mechanism of phagocytosis of chicken thymocytes by mouse and guinea pig macrophages. Microbiol Immunol. 1980; 24:969–979. [PubMed: 6970322]

Tomashefski, J., Farver, C. Anatomy and histology of the lung. Dail and Hammar's Pulmonary Pathology: Volume I: Nonneoplastic Lung Disease. Tomashefski, J.Cagle, P.Farver, C., Fraire, A., editors. Springer Science+ Business Media LLC; New York: 2008. p. 19-48.

Treuel L, Jiang X, Nienhaus GU. New views on cellular uptake and trafficking of manufactured nanoparticles. J R Soc Interface. 2013; 10:20120939. [PubMed: 23427093]

Vranic S, Boggetto N, Contremoulins V, Mornet S, Reinhardt N, Marano F, Baeza-Squiban A, Boland S. Deciphering the mechanisms of cellular uptake of engineered nanoparticles by accurate evaluation of internalization using imaging flow cytometry. Part Fibre Toxicol. 2013; 10:2. [PubMed: 23388071]

Wang C, Yu X, Cao Q, Wang Y, Zheng G, Tan TK, Zhao H, Zhao Y, Wang Y, Harris D. Characterization of murine macrophages from bone marrow, spleen and peritoneum. BMC Immunol. 2013; 14:6. [PubMed: 23384230]

Xia T, Kovochich M, Brant J, Hotze M, Sempf J, Oberley T, Sioutas C, Yeh JI, Wiesner MR, Nel AE. Comparison of the abilities of ambient and manufactured nanoparticles to induce cellular toxicity according to an oxidative stress paradigm. Nano Lett. 2006; 6:1794–1807. [PubMed: 16895376]

Europe PMC Funders Author Manuscripts

Europe PMC Funders Author Manuscripts

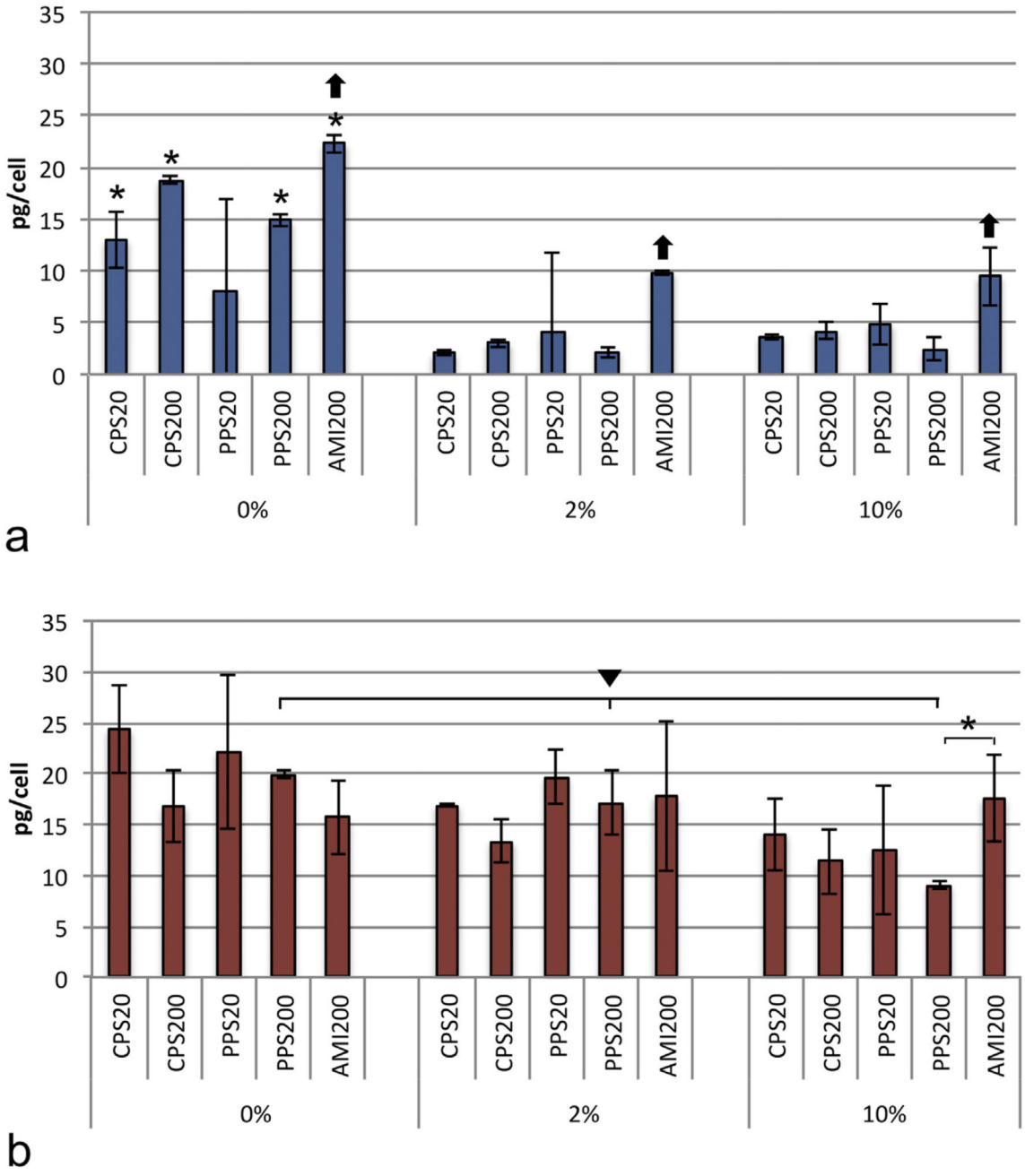

Fig. 1.

Uptake of particles suspended in DMEM + 0% FBS, DMEM + 2% FBS and DMEM + 10% FBS by A549 cells (a) and DMBM-2 macrophages (b) and analyzed by plate reader. Significant differences between DMEM + 0% FBS and media with different FBS content are indicated by asterisks and differences between DMEM + 0% FBS, DMEM + 2% FBS and DMEM + 10% FBS by triangle. Differences in the uptake of one particle compared to all other particles in a given medium are marked with arrow. Data from PPS20 particles were excluded from the analysis due to untypically high variation of the signals (n = 9).

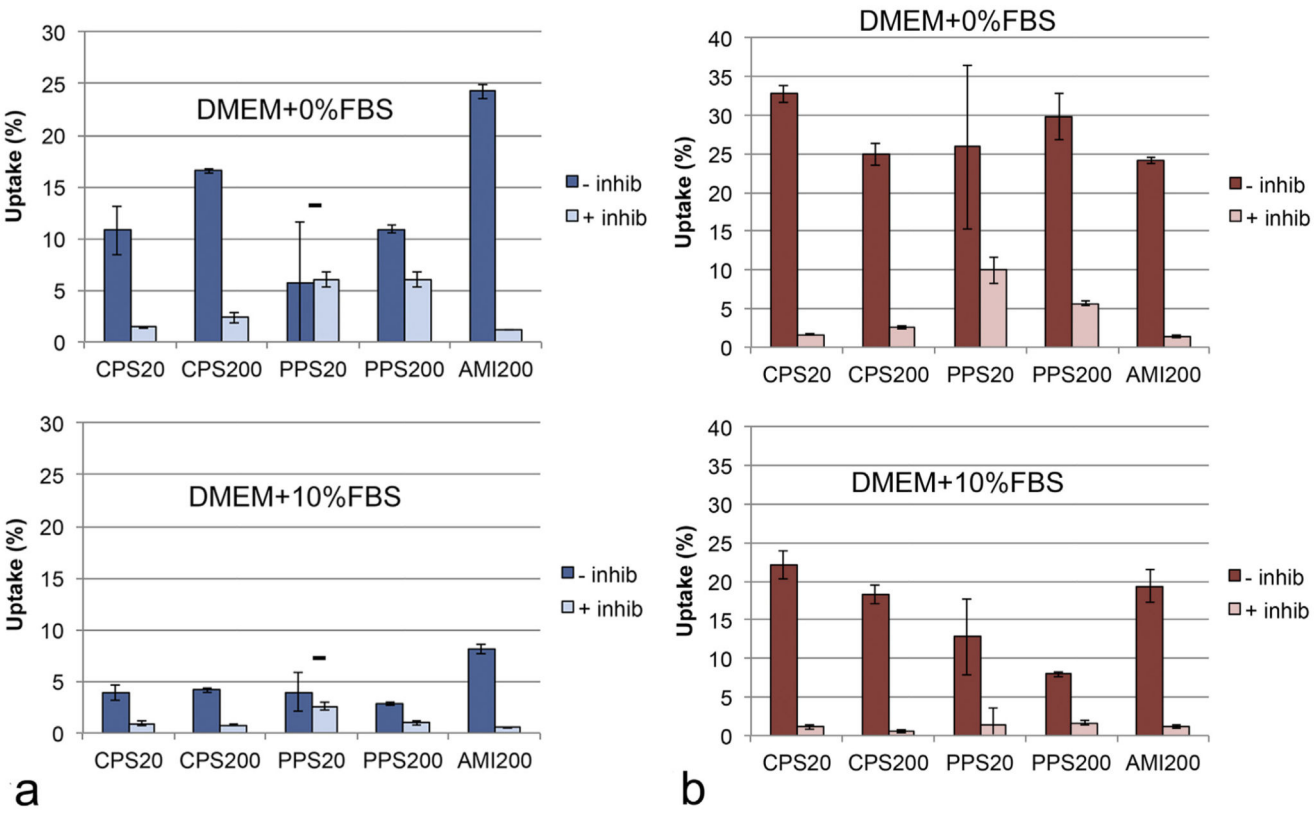

Fig. 2.

Uptake of particles suspended in DMEM + 0% FBS and DMEM + 10% FBS by A549 cells (a) and DMBM-2 macrophages (b) without inhibition and in the presence of 50 mM sodium azide at 4 °C. Evaluation by plate reader with correction of the lower number of cells recovered after the exposure in the inhibitor experiments and normalized to the amount of the particles added to the cells as 100% (n = 3). Inhibition was significant with the exception of PPS20 particles in the exposures to A549 cells.

Europe PMC Funders Author Manuscripts

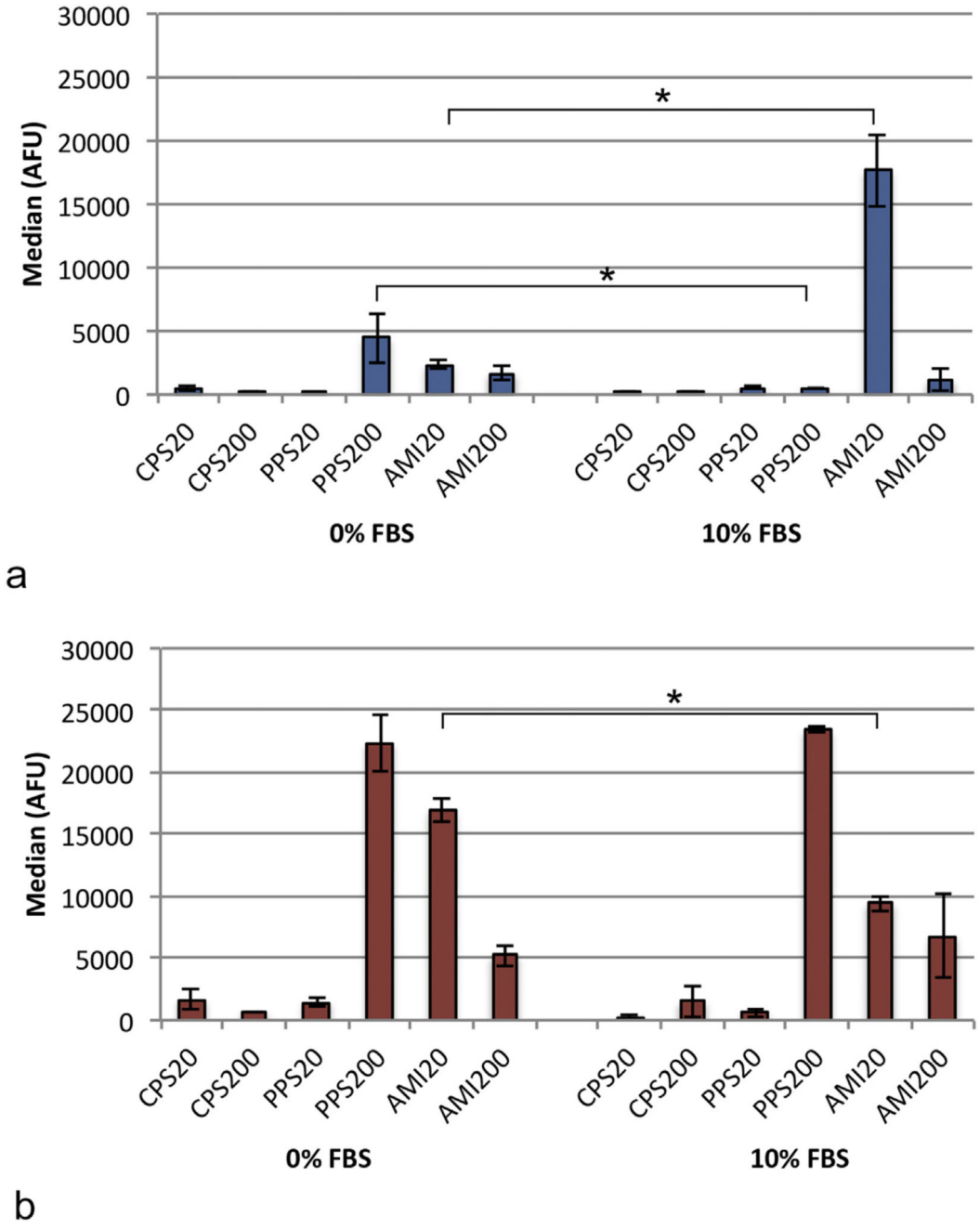

Fig. 3.

Median of fluorescence in the analysis by flow cytometry in A549 cells (a) and DMBM-2 macrophages (b). Significant differences between the uptakes in DMEM + 0% and DMEM + 10% FBS are marked with asterisks (n = 9).

Europe PMC Funders Author Manuscripts

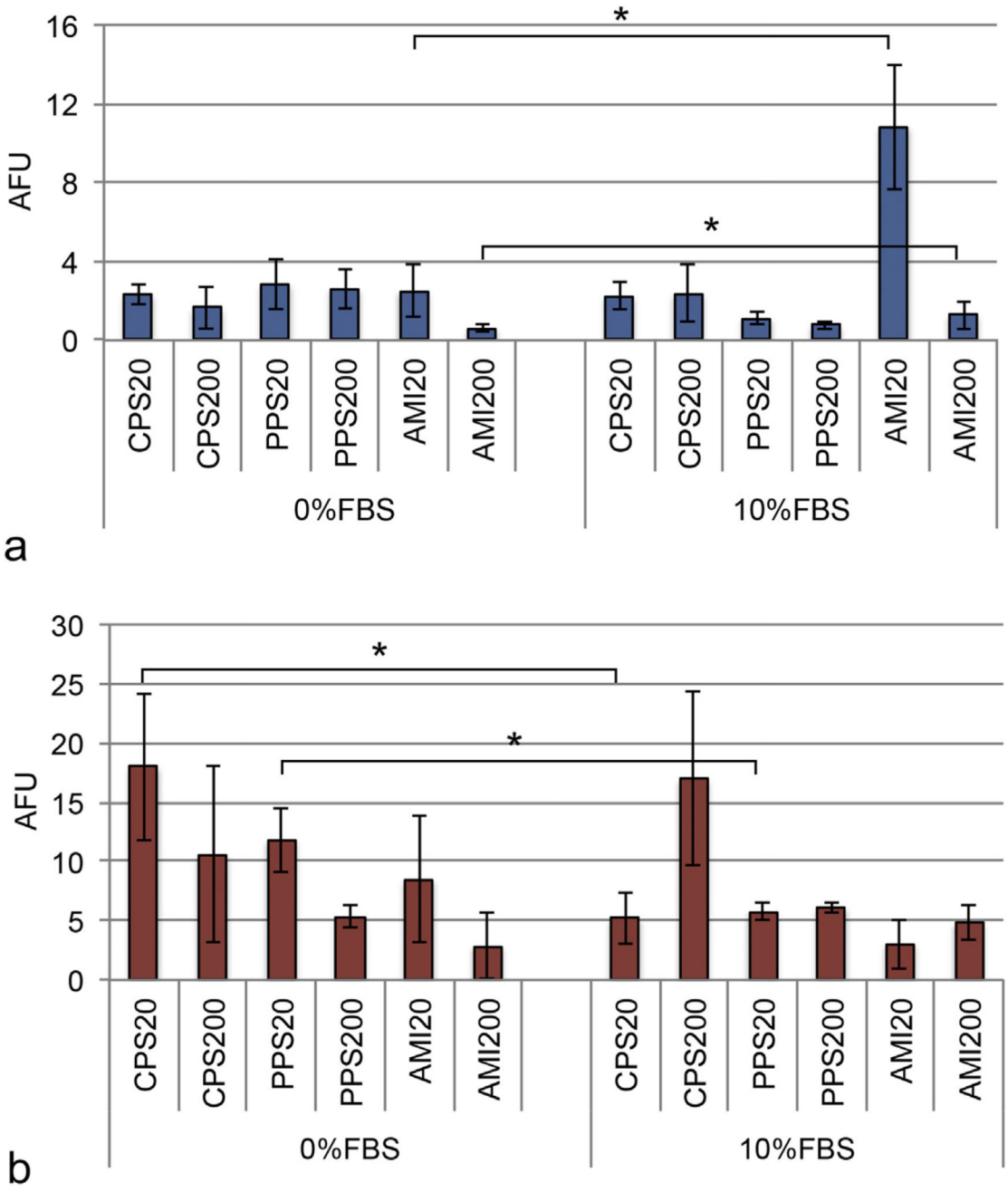

Fig. 4.

Particle uptake in A549 (a) and DMBM-2 (b) cells seeded at low density (4×10^4 cells/chamber) analyzed with image analysis (ImageJ). AFU, arbitrary fluorescence units (n = 4).

Europe PMC Funders Author Manuscripts

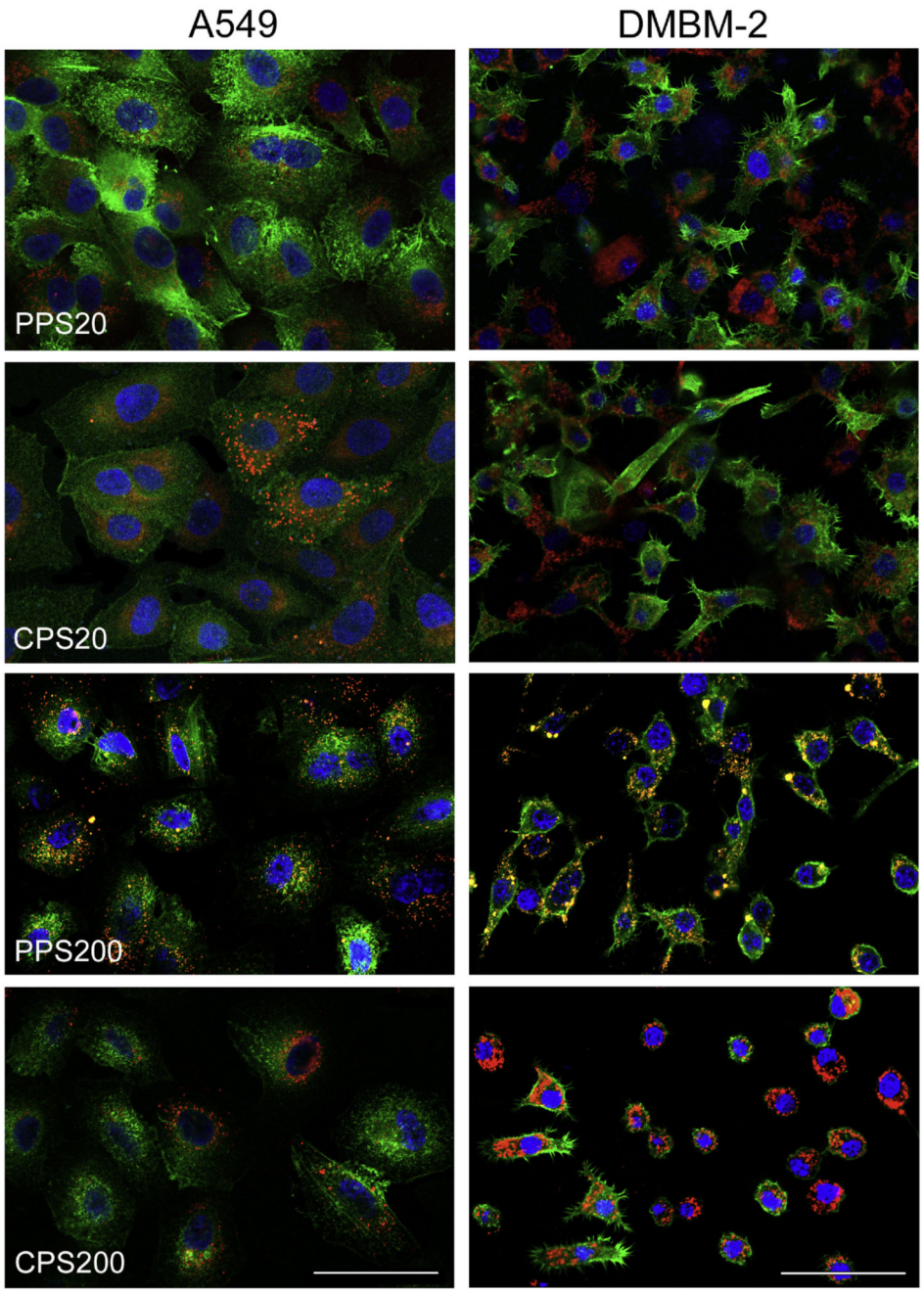

Fig. 5.

Cellular localization of particles after exposure in DMEM + 0% FBS for 24 h. Cells are identified by staining of actin with Alexa Fluor® 488-phalloidin (green) and particles are seen in red. Nuclei are counterstained with Hoechst 33342 (blue). Co-localization is indicated by yellow color. The intracellular localization of particles is easier to discern in A549 cells because the cells are larger and intensity of the phalloidin staining higher. Scale bar: 50 μm. (For interpretation of the references to colour in this figure legend, the reader is referred to the web version of this article.)

Europe PMC Funders Author Manuscripts

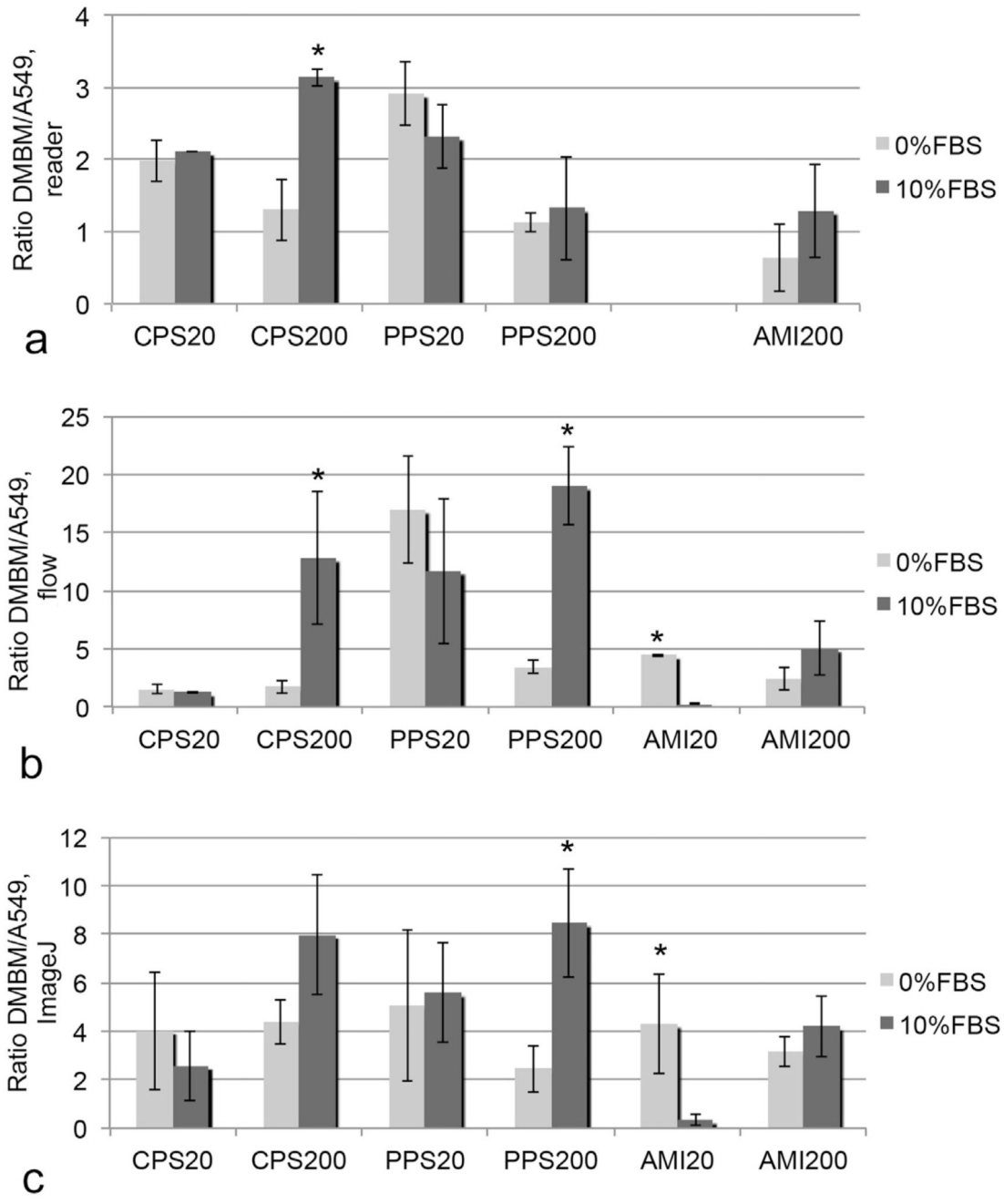

Fig. 6.

Ratios of DMBM-2/A549 uptake determined by different techniques (a: plate reader, b: by flow cytometry and c: image analysis). Significant differences between the exposure conditions are marked by asterisk.

Europe PMC Funders Author Manuscripts

Table 1

Hydrodynamic sizes given as average size (mean ± SD,nm) of particles in cell culture medium (DMEM) with different FBS content (n = 3).

Particle	DMEM + 0%FBS	DMEM + 2%FBS	DMEM + 10%FBS
CPS20	60 ± 21	82 ± 17	96 ± 42
CPS200	236 ± 15	402 ± 159	212 ± 38;952 ± 162 (70%;30%)
PPS20	45 ± 1	60 ± 4	58 ± 10
PPS200	209 ± 3	221 ± 8	224 ± 6
AMI20	25 ± 8;626 ± 259 (70%;30%)	26 ± 7;284 ± 102 (70%;30%)	54 ± 35;523 ± 318 (70%;30%)
AMI200	1415 ± 31	2083 ± 118	1610 ± 217
AMI200, 24h	479 ± 45	373 ± 242	490 ± 214

CPS20: 20 nm carboxyl-functionalized polystyrene particles; CPS200: 200 nm carboxyl-functionalized polystyrene particles; PPS20: 20 nm non-functionalized plain polystyrene particles; PPS200: 200 nm non-functionalized plain polystyrene particles; AMI20: 20 nm amine-functionalized polystyrene particles; AMI200: 200 nm amine-functionalized polystyrene particles.